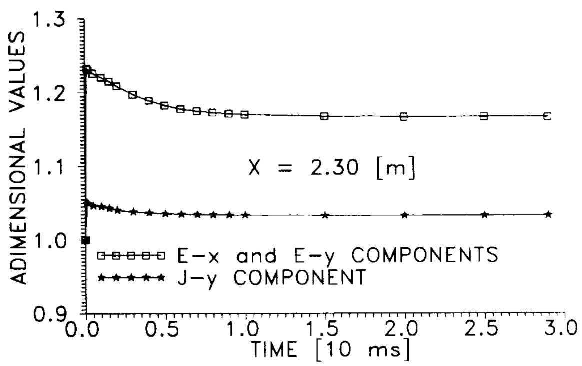

Fig. 8. Time behaviors of the axial and transverse components of the electric field and of the transverse current density component at one third of the channel length.

transient the supersonic flow regime is maintained. The adimensional values of the local velocity plotted in the graphs refer to their initial values (assumed at $t = 0$). A relaxation time of the order of 0.5 ms is observed in the inlet and in the central regions of the duct. In the outlet region a longer time is necessary to reach a stationary flow regime. This phenomenon is related to the change in the distribution of the body force ($\vec{J} \times \vec{B} = J_y B$) following the variation of the current density distribution along the channel. In the inlet region a quite large decrease of the absolute value of the current density y component is observed as shown in Fig. 6. In the central region an increase of J_y caused by the transient is shown. As a consequence, opposite velocity variations are induced in the inlet and in the central regions of the channel. In the outlet region there is no significant variation of current density. The smooth oscillations of the velocity and of the pressure behaviors in the outlet are caused by the necessity to satisfy the pressure boundary condition (see Figs. 5 and 7). The time behaviors of the stagnation pressure at the channel exit, when calculated by means of the three different methods described above, are shown in Fig. 7. The discrepancies of the final values are due to the slightly different locations in which the outlet boundary conditions are imposed. In this region a relaxation time of about 4 ms is calculated by all methods. The time behaviors of the axial and transverse components of the electric field and of the transverse current density at one third of the channel length are shown in Fig. 8. After the transient the absolute values of E_x, E_y, and J_y are found to be increased.

In the examined case Casulli's algorithm utilizes the shortest CPU time to perform the calculations. This is due to the large time step it can use without losing numerical stability. Nevertheless Casulli's method has proved to be as accurate as the methods of MacCormack and Godunov. Even better performance of Casulli's algorithm is expected in the subsonic flow regime as the numerical stability condition of the method allows larger time steps when the flow velocity becomes smaller.

VII. Conclusions

Mathematical models for the analysis of an MHD linear channel have been presented. In order to analyze critical regions of the channel a two-dimensional model has been set up. This model accounts for the divergence of the duct. For the transient analysis a quasi-one-dimensional time-dependent model has been set up. Its numerical solution is obtained through Casulli's algorithm, MacCormack's algorithm, or Godunov's algorithm. These models have been utilized for the analysis of a 230 MW gas-fired MHD generator channel. The scheme developed from Casulli's new semi-implicit method has been found to be less CPU time consuming and to be as accurate as MacCormack's and Godunov's methods.

References

[1] C. A. Borghi, A. Massarini, G. Mazzanti, and P. L. Ribani, "One- and two-dimensional models for a linear MHD generator channel design," in *Proc. 28th Symp. EAM* (Chicago, IL), 1990, pp. 2.8.1–18.

[2] F. J. Zelesznik and S. Gordon, "Calculation of complex chemical equilibria," *Ind. Eng. Chem.*, vol. 60, no. 6, pp. 27–57, 1968.

[3] S. V. Patankar, *Numerical Heat Transfer and Fluid Flow.* New York: Hemisphere Publishing, 1980.

[4] V. Casulli, "Eulerian–Lagrangian methods for the Navier–Stokes equations at high Reynolds number," *Int. J. Numer. Meth. Fluids*, vol. 8, pp. 1349–1360, 1988.

[5] M. Ishikawa and J. Umoto, "New approach to calculation of 3D flow in MHD generators," in *Proc. 22th Symp. EAM* (Starkville, MS), 1983, pp. 2.8.1-18.

[6] W. P. Jones and B. E. Launder, "The prediction of laminarization with a two-equation model of turbulence," *Int. J. Heat and Mass Transfer*, vol. 15, pp. 301–314, 1972.

[7] R. W. MacCormack, "The effect of viscosity in hypervelocity impact cratering," in *Proc. AIAA Hypervelocity Impact Conf.*, 1969, paper 69-354.

[8] M. Holt, *Numerical Methods in Fluid-dynamics.* New York: Springer-Verlag, 1977, ch. 2.

Measurements of the Perpendicular Width of Ionization-Produced Double Layers

Bin Song, R. L. Merlino, and N. D'Angelo

Abstract— **Measurements of the perpendicular (to B) double-layer widths of ionization-produced (anode) double layers are presented. These widths were determined from measurements of the double-layer charge separations. The variations of the transverse-to-B widths with plasma density and magnetic field strength are given.**

I. Introduction

In magnetized plasmas, double layers may be formed having segments with the electric field parallel to the magnetic field and segments with the electric field perpendicular to the magnetic field. One interesting question is what determines the width of the double layer in the direction transverse to the magnetic field [1], [2]. A related question concerns the effect of a magnetic field on the transition layer between a plasma and an absorbing wall [3]. In the direction along the magnetic field, it is often stated that the width is determined by the Debye length, λ_D, and experimental measurements indicate that the field-aligned double-layer thicknesses are on the order of tens to hundreds of λ_D's.

Manuscript received October 21, 1991; revised February 11, 1992. This work was supported by ONR and NASA.

The authors are with the Department of Physics and Astronomy, University of Iowa, Iowa City, IA 52242.

IEEE Log Number 9201366.

0093-3813/92$03.00 © 1992 IEEE

There have been only a few laboratory experiments in which the question of the transverse double-layer width has been examined. Jovanovic *et al.* produced fully three-dimensional double layers by introducing an electron beam along the axis of a magnetized cesium Q machine plasma column [4]. They mapped out the two-dimensional double-layer equipotential contours for magnetic field strengths of 1000, 1800, and 3400 G. These measurements indicated that the transverse-to-$\boldsymbol{B}$ scale length of the double layers was roughly given by the ion gyroradius.

The question of the scaling of the double-layer width both along and perpendicular to the magnetic field was also addressed in the experiments of Alport *et al.* [5] and Cartier and Merlino [6]. In these experiments double layers were produced by drawing a discharge to an anode plate located in the diverging magnetic field region of a weakly ionized argon plasma column. If the anode voltage was above the argon ionization potential, the anode sheath developed into a strong, three-dimensional double layer. The magnetic-field-aligned portion of the double layer had a thickness which decreased as the plasma density increased, suggesting a Debye length scaling. The transverse double-layer thickness was of the order of the thermal ion gyroradius.

II. Experimental Results

This note provides further experimental results on the thickness of the double layer in the transverse-to-$\boldsymbol{B}$ direction. The double layers were produced in a manner similar to that described above [4]–[6], although the device used was a single-ended Q machine operated with a potassium plasma. A schematic diagram of the device is shown in Fig. 1(a). A K^+ plasma is produced by contact ionization of potassium atoms from an atomic beam oven (not shown) on a 6-cm-diameter tantalum plate (HP) heated to about 2300 K by electron bombardment. The plasma is confined radially by a magnetic field produced by two sets of field coils (EAST and WEST) which can be energized separately. For the experiments described here only the east coils are energized so that a diverging magnetic field geometry is obtained (see Fig. 1(b)). A 6-cm-diameter cold anode plate is located 65 cm from the hot plate, in the region of diverging magnetic field. The magnetic field strength at the cold plate is about 1/10 of the value at the hot plate. The diameter of the K^+ plasma column increases as the plasma flows into the diverging magnetic field region; the boundary of the plasma column coincides roughly with the magnetic flux tube which intersects the hot plate and the floating end plate, as illustrated schematically in Fig. 1(b).

To produce the double layers, the system was filled with argon gas at a pressure $\sim 5 \times 10^{-4}$ torr, and the anode plate biased at 50–80 V positive. The stable, fully three-dimensional V-shaped double layers (shaded region in Fig. 1(b)) evolve from the anode sheath, and are maintained by ionization caused by the electrons (from the potassium plasma) which are accelerated through the potential gradient. Since the potential gradient is typically several tens of volts, no K^+ ions can penetrate it. Thus the high-potential region contains only Ar^+ ions. Because of the divergence of the magnetic field lines, the K^+ plasma-column radius at the anode plate location is roughly 10 cm. When the double layer structure is formed, the Ar^+ ions produced within the high-potential region can flow back through the double layer into the low-potential region. Thus, when the double layers are present, the main plasma column is populated by both K^+ and Ar^+ ions. Further details on the properties of these double layers and the effects of varying the magnetic geometry have been presented elsewhere [7].

The transverse-to-$\boldsymbol{B}$ double-layer widths were determined from emissive probe measurements of the radial profiles of the plasma potential. A typical example of a radial potential profile taken 2 cm in front of the anode plate, where the magnetic field strength was

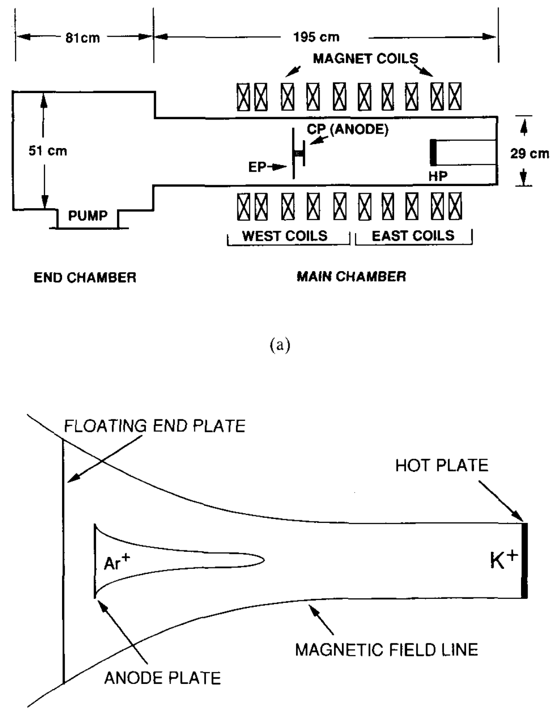

Fig. 1. (a) Schematic of the experimental setup. For this study only the EAST coils were used so that the magnetic field was diverging toward the anode plate. (b) Schematic configuration used for the production of anode double layers in a diverging magnetic field.

385 G, is shown in Fig. 2(a). In this case the neutral argon pressure was 6×10^{-4} torr, and the anode plate voltage and current were $V_P = 80$ V and $I_P = 40$ mA respectively. To determine the double-layer width from this profile, a polynomial fit (typically 20th order) is made to the data. This fit is shown as the solid line in Fig. 2(a). Given the fitted function $V(r)$ we obtain the electric field, $E = -dV/dr$, shown in Fig. 2(b), and the double-layer charge density, $\rho \sim dE/dr$, shown in Fig. 2(c). The double-layer width is then taken as the center-to-center radial separation between the positive charge layer and the negative charge layer. For example, the measured width for Fig. 2(c) is 7–8 mm.

Using this method we next investigated the dependence of the transverse-to-$\boldsymbol{B}$ width on the plasma density and magnetic field strength. The plasma density in a Q machine can be varied by changing the hot plate temperature. By raising or lowering the plasma density the anode plate current is increased or decreased. Fig. 3 shows the variation of the transverse-to-$\boldsymbol{B}$ width with anode plate current (density). These data were taken 5 cm in front of the anode plate with $B = 210$ G, $P = 5 \times 10^{-4}$ torr, and $V_P = 80$ V. Although the plasma density was varied by roughly an order of magnitude, the width essentially did not change. Over this range of densities the double-layer potential drop varied by only 10%.

Finally, the dependence of the width on magnetic field strength at fixed plasma density was examined. Radial potential profiles, taken 5 cm in front of the anode plate, are shown in Fig. 4 for various magnet coil currents. From data of the type shown in Fig. 4 the perpendicular widths were determined using the method described previously. Fig. 5 shows a plot of the perpendicular widths versus the magnetic field strength. For comparison the argon ion gyroradii

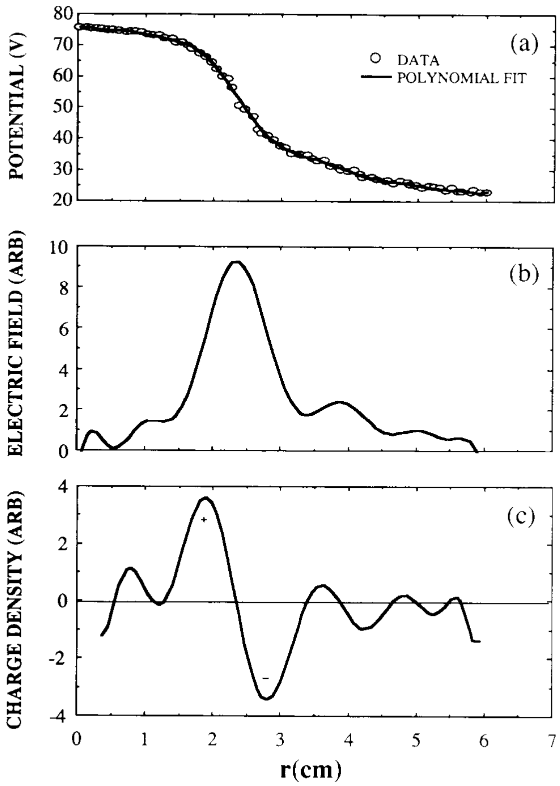

Fig. 2. Radial profiles of (a) plasma potential, (b) electric field, and (c) charge density taken 2 cm in front of the cold anode plate with $P = 6 \times 10^{-4}$ torr, $V_P = 80$ V, and $I_P = 40$ mA. The magnetic field strength at the position of the measurement was 385 G. The electric field and the charge density were obtained from the polynomial fit to the data in (a).

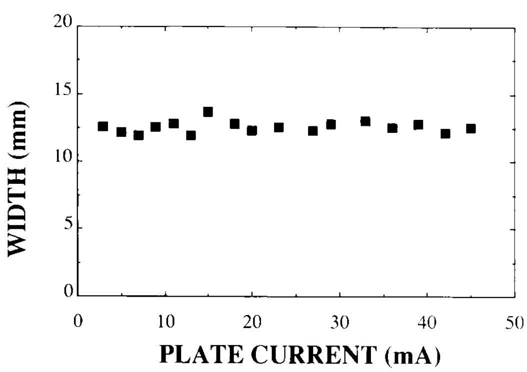

Fig. 3. Variation of the transverse-to-B width with plate current. The variation of the plate current from ~ 5 mA to ~ 45 mA represents a plasma density variation of about one order of magnitude. Measurements were taken 5 cm in front of the cold anode plate with $P = 5 \times 10^{-4}$ torr and $V_P = 80$ V. At the measurement position $B = 210$ G.

for $T_i = 0.2$ eV are shown as the solid line. The measured widths are of the order of the gyroradii of the 0.2 eV thermal argon ions in the high-potential region. Since all ions in the high-potential region must be produced locally by ionization, using $T_i = 0.2$ eV for the

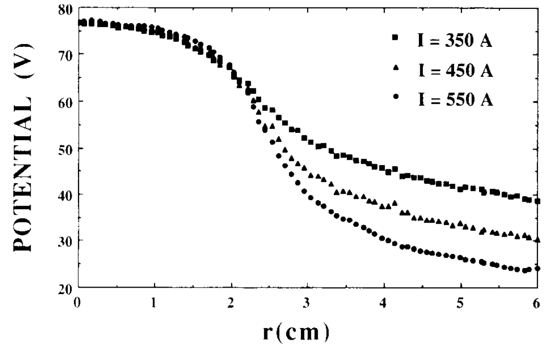

Fig. 4. Radial profiles of the plasma potential for various magnetic field strengths (coil currents). Here $P = 5 \times 10^{-4}$ torr, $V_P = 80$ V, and $I_P = 40$ mA.

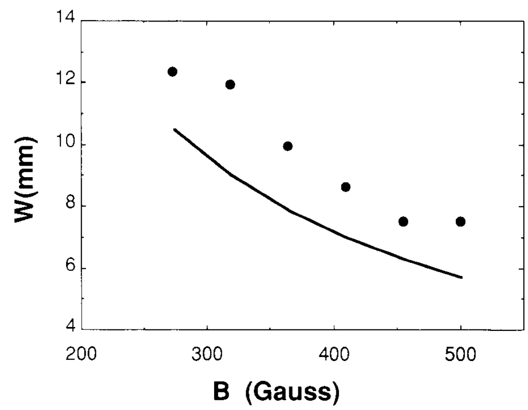

Fig. 5. Variation of the transverse-to-B width with magnetic field strength at constant plasma density. The measurements were taken 5 cm in front of the anode plate. Solid line: Ar^+ ion gyroradii for $T_i = 0.2$ eV.

Ar^+ ions is appropriate since this is a typical value for the ion temperature in low-pressure discharge plasmas. For magnetic field strengths below about 300 G, the measured widths do not continue to increase as fast with decreasing B-field strength. This is most likely due to the decreasing degree of magnetization of the Ar^+ ions as B is reduced. For example, for $B \cong 100$ G and $p \approx 10^{-3}$ torr we estimate $\nu_{in}/\omega_{ci} \lesssim 1$, where ν_{in} is the ion–neutral collision frequency and ω_{ci} is the ion gyrofrequency.

III. Conclusions

In summary, we have presented measurements of the width of an ionization-produced double layer in the direction perpendicular to the magnetic field. These transverse-to-$\boldsymbol{B}$ widths do not exhibit any dependence on plasma density, but do seem to follow, at least at the higher magnetic field strengths, a $1/B$ scaling. These results are in general agreement with previous experiments.

References

[1] D. W. Swift, "On the formation of auroral arcs and acceleration of auroral electrons," *J. Geophys. Res.*, vol. 80, pp. 2096–2108, 1975; "An

equipotential model for auroral arcs: The theory of two-dimensional laminar electrostatic shocks," vol. 84, pp. 6427–6434, 1979.

[2] J. E. Borovsky and G. Joyce, "Numerically simulated two-dimensional auroral double layers," *J. Geophys. Res.*, vol. 88, pp. 3116–3126, 1983; J. E. Borovsky, "The scaling of oblique plasma double layers," *Phys. Fluids*, vol. 26, pp. 3273–3278, 1983.

[3] R. Chodura, "Plasma-wall transaction in an oblique magnetic field," *Phys. Fluids*, vol. 25, pp. 1628–1633, 1982.

[4] D. Jovanovic *et al.*, "Three dimensional double layers in magnetized plasmas," *Geophys. Res. Lett.*, vol. 9, pp. 1049–1052, 1982.

[5] M. J. Alport, S. L. Cartier, and R. L. Merlino, "Laboratory observations of ion-cyclotron waves associated with a double layer in an inhomogeneous magnetic field," *J. Geophys. Res.*, vol. 91, pp. 1599–1608, 1986.

[6] S. L. Cartier and R. L. Merlino, "Anode-type double layers in a nonuniform magnetic field," *Phys. Fluids*, vol. 30, pp. 2549–2560, 1987.

[7] B. Song, R. L. Merlino, and N. D'Angelo, "The effect of a magnetic field gradient on anode double layers," *Physica Scripta*, vol. 45, pp. 395–398, 1992.